Journal of Power Sources 247 (2014) 189–196

Contents lists available at ScienceDirect

Journal of Power Sources

journal homepage: www.elsevier.com/locate/jpowsour

Evaluation of mechanical abuse techniques in lithium ion batteries

Joshua Lamb*, Christopher J. Orendorff

Power Sources Technology Group, Sandia National Laboratories, United States

HIGHLIGHTS

- We examined mechanical techniques to generate internal short circuits in Li-Ion cells.
- Multiple test conditions and cell constructions were evaluated.
- Post-mortem analysis was performed using CT imaging.
- Results were found to vary significantly with test conditions and cell construction.

ARTICLE INFO

Article history:
Received 3 December 2012
Received in revised form
22 June 2013
Accepted 16 August 2013
Available online 31 August 2013

Keywords:
Li-Ion
Lithium ion
Battery
Safety
Internal short circuit
Mechanical abuse

ABSTRACT

Mechanical tests are a commonly used method for evaluating the safety performance of batteries. The mechanical blunt rod testing method, as well as sharp nail penetration, was performed on commercially available cells. Evaluation was carried out on different cell constructions as well as varying test conditions. Results obtained at ambient conditions were found to differ little from traditional sharp nail penetration testing. When tested at elevated temperatures it was observed that the results became heavily dependent upon the internal construction of the cell. Computed Tomography (CT) imaging confirmed this, showing differences in behavior depending on whether or not a solid core was used in the cylindrical cell construction. Pouch cells were tested as well, showing that a full penetration of the cell was necessary to initiate a failure event within the cell.

1. Introduction

Lithium ion batteries have been in use in the consumer electronics industry for well over a decade. Further, they are increasingly being applied to vehicular and stationary energy storage applications. In this time awareness of potential safety issues has increased dramatically [1–4]. Field failures of lithium ion batteries in consumer electronics devices have been well documented and prompted several large scale recalls of product. In nearly all cases, field failure was the result of an internal short circuit developed over the course of normal use. Several causes have been identified including mechanical defects introduced during manufacturing, small impurities trapped between the electrode layers and dendritic growth of lithium or other metallic particles bridging the electrodes [2,5,6]. Because these develop and progress over time, and are extremely rare, quality control at the point of manufacture is generally unable to detect these faults. This leaves the option of understanding and mitigating the consequence of internal short circuit failures. Traditionally, mechanical intrusion of a cell, such as through nail penetration, has been used as a method to simulate an internal short circuit. However, recent work has shown that these methods are not entirely representative of most spontaneous internal short circuits [7–10]. However, while significant work has been performed to develop more appropriate testing methods, a general consensus on methods to initiate internal short circuits has not been reached. Because of this, many testing laboratories continue to use mechanical methods as a substitute for a broadly accepted internal short circuit test. Further, the usage conditions of lithium ion batteries are continually evolving. Testing and evaluation of batteries for consumer electronics devices has typically focused on the impacts of spontaneous failure of the cells, or the impacts of electrical and thermal abuse as severe mechanical damage was unlikely. Physical damage to a cell that is relatively unlikely in a consumer electronics device is an eventuality that

* Corresponding author. Tel.: +1 (505) 284 9709.
E-mail address: jlamb@sandia.gov (J. Lamb).

0378-7753/$ – see front matter © 2013 Elsevier B.V. All rights reserved.
http://dx.doi.org/10.1016/j.jpowsour.2013.08.066

must be prepared for in mass produced electric vehicles. This leads to an importance to more fully understand the nature and impacts of mechanical testing. The work presented here is to better understand the nature of mechanical abuse testing, such as its reliability, the impact of varying test conditions and the impact of differing cell constructions. It does not attempt to make an evaluation of the suitability of mechanical testing as an internal short circuit test.

Nail penetration tests of Li-Ion cells, where the cell is rapidly punctured with a sharp nail, have long been used as an abuse test [11]. Further, without a strong standard for internal short circuit tests, they are used as a stand in to simulate an internal short as well. This is considered problematic due to the fairly complex nature of battery internal short circuits. Internal short circuits have been observed to occur from anode to cathode, anode to Al current collector, cathode to Cu current collector, and between the Al and Cu current collectors, with varying results [9,10,12–15]. Nail penetration creates a relatively large shorting volume with multiple electrode layers brought into electrical contact with one another as well as shorting through the nail, plus significant immediate damage to the cell. This creates a very non-localized electrical pathway, with the failure caused by the nail occurring over a fairly large volume. Other forms of mechanical abuse, such as flat crushing and three point bend tests have been studied by Greve and Fehrenbach [16] as well as Sahraei et al. [17], finding that failures in these conditions typically arise from macroscopic damage to the electrodes, such as large cracks through the electrode jelly roll or delamination of electrode layers. Typical field failures, meanwhile, rise from relatively small defects and begin as a very localized process. Among other effects, this leads field failures to have a relatively high impedance (at least initially) and concentrate the related heat generation in a very small volume when compared to the failure caused by a sharp nail penetration [10,12,13,15]. This has led to the development of various tests to try and simulate internal short circuits within Li-Ion cells.

Several tests have been developed that use some sort of mechanical deformation to damage the cell, the most well-known of which being the aforementioned nail penetration test. Other mechanical techniques attempt to deform the cell enough to cause a failure without causing significant physical damage to the cell. Researchers at Oak Ridge National Laboratory and Motorola [7,8] have developed such a test for prismatic pouch cells that attempts to create a short circuit between the anode and cathode by compressing a point of the cell between two spheroids. Some attempts have been made to generate internal shorts using more representative non-mechanical methods. Orendorff et al. [9] at Sandia National Laboratories have proposed using an insert of a low melting point metal to generate a controllable short circuit by slightly elevating the temperature of a cell. Researchers at TIAX LLC have reported a method of generating shorts by depositing metallic defect particles in a cell and growing them dendritically through battery cycling [10]. Such testing methods represent the ongoing work to develop a true internal short circuit test applicable to lithium ion cells.

The method used in this work was first developed by Underwriters Laboratories and NASA [12,18] and creates a failure by mechanically deforming a cell with a blunt rod. This attempts to simulate an internal short circuit by applying force normal to the axis of a cylindrical cell sufficient to cause the outer electrode layers to come into contact with one another and short but without doing significant damage cell itself. The objective of this work is to evaluate this method under different test conditions and battery constructions as well as expand on the method by evaluating its applicability to different cell orientations and cell types. Testing was performed on commercially available 18650 and pouch cells.

2. Experimental

Experiments were performed on commercially obtained 18650 Li-Ion batteries and pouch cells. Cell A is a LG 2200 mAh cell, model ICR18650 S3. Cell B is a Panasonic 2200 mAh cell, model CGR18650CG. The pouch cells used are 3000 mAh cells from AA Portable Power Corp (model PL-7035130-10C), purchased at www.batteryspace.com. These cells use collocated current tabs and have dimensions of 7.4 mm × 35.5 mm × 130 mm. Computed Tomography (CT) scans were used to evaluate the internal structures of the cells before testing and can be seen in Fig. 1. The most prominent difference observed between the two cells is that type B (Fig. 1 right) has an easily observed solid core present in the center of the spiral wound cell. Both cell types at 100% state of charge have a nominal capacity of 2200 mAh and cell voltage of 4.2 V. Cell type A (Fig. 1 left) used proprietary mixed metal oxide cell chemistry, while cell type B as well as the prismatic pouch cell evaluated used $LiCoO_2$ based cell chemistry. Computed tomography imaging was performed with a Northstar Imaging CT X50 with microfocus capability.

Blunt rod indentation and puncture was performed using a 3 mm diameter (nom.) stainless steel blunt rod. The blunt rod is mounted to a hydraulically driven actuator with a stroke of 9 inches and a maximum applied load of 10,000 lbf. Tested batteries were held in place with brass fixtures, insulated to prevent electrical contact from the cell can to the fixture and fitted with cartridge style heaters to allow testing at elevated temperatures. Two fixtures

Fig. 1. CT imaging showing the internal construction of cell type A (left) and B (right). The primary observable difference is the presence of a solid core in type B, while in type A the center of the cell is left empty.

were used allowing force to be applied both along and across the axis of the cylindrical battery and can be seen in Fig. 2.

Tested cells were deformed at a rate of 2 mm min^{-1} until the rod punctured through to the opposite side of the can or a voltage drop of at least 100 mV was observed. This rate was used to allow the indentation to be halted once the voltage drop was observed. The voltage and temperature were monitored until the battery returned to ambient conditions. Cylindrical cells were tested in directions normal and parallel to the cell axis. The objective of indentation normal to the axis is to sufficiently compress the electrode layers such that they break through the separator and come into contact with each other causing an internal short. Indentation parallel to the axis, meanwhile, attempts to effectively create a short by deforming the negative can until it comes into contact with either the positive electrode or current collector to create a short circuit. Prior to testing, all cells are imaged to determine the location of the negative tab and weld points to the can. All cells are tested at load points that are 90° from the tab in both test orientations.

Traditional nail penetration testing was also carried out on these two cell types using a 3 mm steel nail sharpened to a fine point. Cells were fully penetrated at a rate of 2 cm s^{-1}. This rate is noticeably different from that used for the indentation tests, but is used to provide a comparison in the reaction of the slow indentation tests to the more traditional nail penetration tests typically used for battery abuse testing that operate at a higher rate of penetration [11].

Pouch cells were also evaluated by indenting normal to the electrode layers and parallel to the electrode layers. Similar to indentation normal to the cylindrical axis, indentation normal to the electrode layers attempts to compress the electrode layers together until they break through the separator and cause an anode–cathode short. Indentation parallel to the electrode layers attempts to partially deform the electrode layers until a short circuit occurs.

Temperature measurement in all cases was taken using a K-type thermocouple mounted to the body of the cell under test. The thermocouple was positioned at the mid-point of the cell body, offset slightly from the point of penetration to prevent interference from the nail. Heating for cells tested at elevated temperature was accomplished by the use of OMEGA cartridge heaters in the brass fixtures used for cell testing.

The cell voltage, cell surface temperature, indenter force and penetrator displacement were measured for each test. The maximum observed indenter force, total penetrator displacement required to reach the above internal short conditions, and maximum observed temperature were noted and are recorded here in Table 1.

3. Results and discussion

Blunt rod indentation was performed in both the axial (parallel to the cylindrical axis) and transverse (normal to the cylindrical axis) directions of cylindrical cells as well as horizontally (through the flat face of the cell) and vertically (through the side of the cell) through prismatic pouch cells. Representative peak temperatures, applied forces and displacement required to cause the short circuit event are listed in Table 1. In the case of the nail penetration tests, a rapid puncture to 20 mm displacement was used to ensure full puncture of the cell.

Blunt rod penetration was applied in the direction of the axis on cell type A, and is shown in Fig. 3. Little effect was seen until the cell can was punctured at 10.7 mm displacement and a peak load of 823 N, however on puncture there was an evident, hard short circuit. Venting of the cell occurred through the burst disk at the positive end of the battery, along with sparking which ignited the electrolyte vapors escaping from the cell. Thermal runaway was evident as well with the cell reaching a maximum temperature of 470 °C. CT imaging of the cell after testing is seen in Fig. 3 (right). This shows that extensive damage to the internal cell components was necessary to cause a failure, with evidence of significant penetration into the electrodes before the short occurred. Also seen is evidence of the melting of electrode materials, seen as small beads collecting outside of the electrode. This is likely the aluminum current collector as it has the lowest melting point of the internal constituent components at 660 °C.

Cell type A was also subjected to blunt rod indentation in the center of the cell normal to the cell axis. The results can be seen in Figs. 4 and 5. Similarly to the axial loading data failure of the cell only occurred once the cell was punctured at 5.4 mm displacement and 935 N. After the exterior was punctured, an abrupt and energetic failure was observed, with the cell venting primarily through the vent at the positive end of the cell. This created a runaway event with a peak observed temperature of 455 °C. Arcing was seen as well both through the blunt rod as well as from the cell vent. The CT imaging shows that significant damage to the cell electrode was done before shorting occurred (Fig. 5). The cross sectional view also shows that the electrode material expanded significantly into the void space in the center of the cell.

A hard short circuit and high rate runaway is the representative failure mode for this transverse blunt rod load test. However, soft shorting behavior has been observed, albeit far less frequent (~<25%). One instance of soft shorting in cell type A conducted under the same conditions as the cell in Figs. 4 and 5 was observed during blunt rod indentation normal to the axis and is shown in Fig. 6. In this case a total displacement of 5.7 mm and load of ~940 N were observed. The data show a voltage drop to ~1.6 V and initial cell heating to 95 °C. When the load rod is retracted and the load removed, the voltage recovers to ~3.1 V and slowly discharges through the soft short. This suggests that the high resistance soft short is localized at the outer layers of the cell roll. This is consistent with the CT imaging showing that the cell can was slightly ruptured

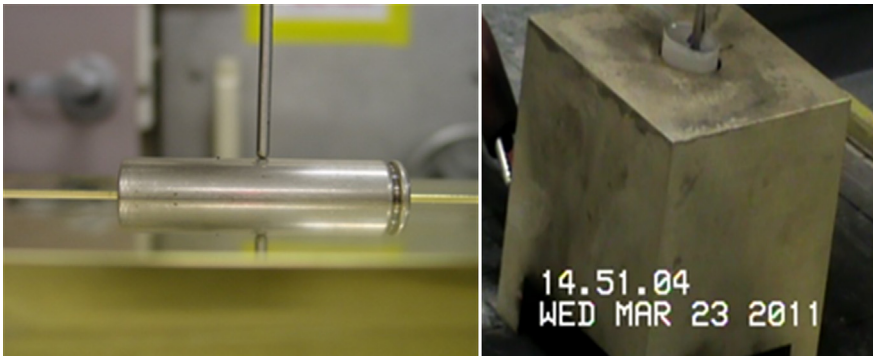

Fig. 2. The blunt rod test fixtures used for testing cylindrical 18,650 cells normal to the axis (left) and parallel to the axis (right). The fixtures also contain embedded heating elements to allow elevating the cell temperature during testing.

Table 1
Representative peak indentation, loads and temperatures for cells and test conditions examined in this study.

Cell type	Test type	Initial temperature	Orientation	Peak force (N)	Total displacement (mm)	Peak temperature (°C)	Failure mode
A	Blunt rod	RT	Axial	823	10.7	470	Hard Short
A	Blunt rod	RT	Transverse	935	5.4	455	Hard Short
A	Blunt rod	RT	Transverse	939	5.7	99	Soft Short
A	Nail penetration	RT	Transverse	191	20	662	Hard Short
A	Blunt rod	60 C	Transverse	819	5.0	115	Soft Short
B	Blunt rod	RT	Transverse	788	4.1	600	Hard Short
B	Nail Penetration	RT	Transverse	89	20	420	Hard Short
B	Blunt rod	60 C	Transverse	623	4.5	330[a]	Hard Short
Pouch	Blunt rod	RT	Horizontal	289	4.2	247	Hard Short
Pouch	Blunt rod	RT	Vertical	490	5.7	200	Hard Short

[a] Energetic eruption of cell contents limit accuracy of maximum temperature reading.

and the short appears to have occurred between electrodes near the outside edge of the electrode. This also shows significant collapse of the electrode into the void at the center of the cell. The primary difference observed between the two failure conditions was the damage done to the electrode material. When a more energetic short circuit is observed the blunt rod was able to penetrate several layers deep into the cell, tearing through several electrode layers. In the less energetic event, the electrode material deformed inward into the central core rather than allowing the indenter to tear through.

Indentation was carried out normal to the axis on cell type B with representative test results shown in Fig. 7. Similarly to cell A, abrupt shorting was observed once the cell can was punctured. The peak temperature was measured to be 600 °C, which is ~150 °C greater than the peak temperature observed for the same test conditions on cell A. This difference in peak temperature could be a function of different cell chemistry. It is well known that different cathode materials give rise to different thermal runaway response, where mixed metal oxide cathode runaway reactions are considerably milder than cobalt oxide cathodes [9,19]. The total displacement of 4.1 mm however was slightly less than that needed to produce a runaway of similar intensity in cell A. The internal imaging of the cell (Fig. 7 right) showed that the central core held the electrodes more or less in place, and that during puncture the electrodes were effectively sandwiched between the indenting rod and the solid core. With the solid core in place less indentation is necessary to achieve sufficient compression of the electrode layers to cause a severe short circuit event. This is illustrated in Fig. 8 which compares the force–displacement behavior of cells A and B. Similar force is required to puncture the can itself, however 1–1.5 mm difference exists in the displacement needed. Cell B shows puncturing of the can (seen as the sharp drop in force on the figure) occurring at 4.05 mm, essentially at the point of short circuit for that cell (4.1 mm, see Table 1). The puncture point of cell A is observed at 5.4 mm where the short circuit event occurs. The mild soft shorting in cell A is observed at 5.7 mm. In both cases the jelly roll was likely able to deform inward into the hollow core, with the primary difference being the damage caused to the electrode layers by the indenter when the can was punctured. While in two of the three cases presented so far the event was ultimately caused by large scale mechanical damage to the cell, these force comparisons are helpful to illustrate how two outwardly similar cells can have different responses to the same mechanical test condition. The presence of the solid core in this case causes the electrodes to be pinched between the blunt rod and the core, while when it was absent the electrodes were able to collapse inward.

Both cell types were tested with fast nail puncture normal to the cell axis for comparative purposes, with results shown in Fig. 9. This data shows similar hard shorting behavior to the tests where the blunt rod fully penetrated the cell. In total, the temperature and voltage data for the cells gives results largely similar to that seen for a traditional nail penetration test regardless of the direction. Somewhat higher peak temperatures were observed for this nail test (662 °C for cell A), but the chief difference seen in the nail

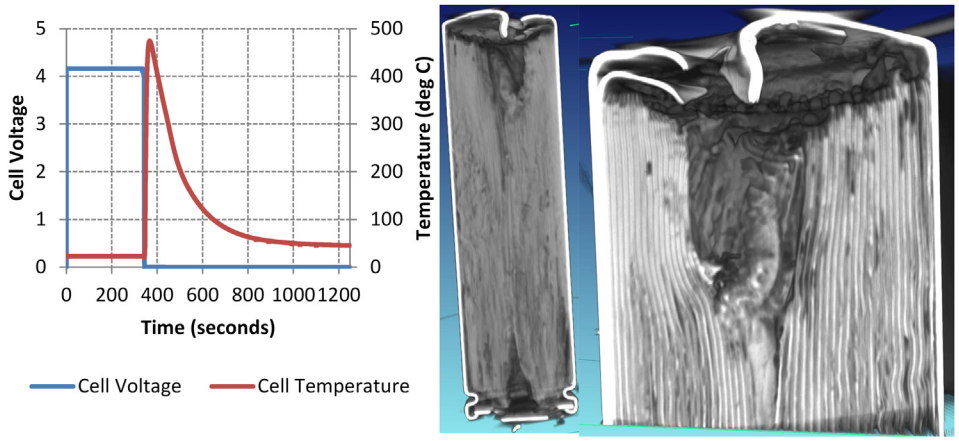

Fig. 3. Cell type A indented parallel to the cell axis until shorting. The shorting observed is abrupt and caused an energetic thermal (left) runaway accompanied by the venting of hot vapors and incandescent particles from the pressure release vent at the positive cap of the cell. The image of the entire cell (middle) shows significant damage to the electrode as a whole, including a collapse into the open central cavity. Imaging near the point of indentation/puncture (right) shows significant damage was necessary to the electrode to cause cell shorting.

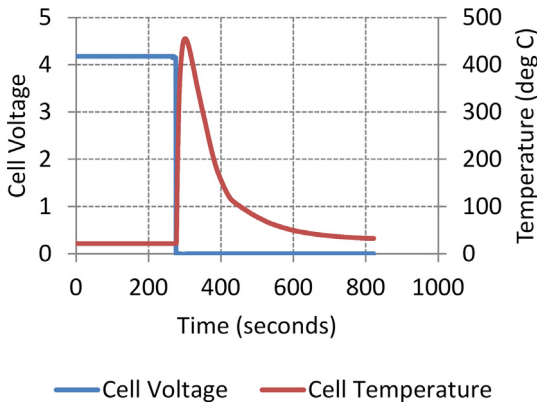

Fig. 4. Cell voltage and temperature data for cell type A indented normal to the cell axis. The observed shorting was abrupt and the maximum temperature seen is similar to that observed for the same cells indented parallel to the axis (Fig. 3).

penetration was that the cell canister was more prone to rupture during the nail penetration tests. This is likely due to additional stresses put onto the can by the rapid nail puncture, as the thermal and electrical behaviors were largely similar. It is also worth noting that the two cells show similar thermal responses, contrary to the higher cell response seen for cell B in the blunt rod testing (Figs. 4–7). This appears to indicate that differences in thermal response are more dependent on factors other than cell chemistries.

Indentation normal to the cell axis was performed on cells heated to 60 °C on both cell types. Cell type A reliably showed less vigorous short circuit events. As can be seen in Fig. 10 (left) the short occurred after minor rupturing of the cell can with only a modest increase in temperature. The peak load and displacement were slightly lower, 819 N and 5.0 mm vs. 939 N and 5.7 mm. At this low displacement, the load observed is likely the force required to deform and ultimately puncture the exterior can. The increased temperature may, however, change the mechanical properties of the constituent components, in particular the polyolefin separator typically used in lithium ion batteries, and creating the observed soft shorting. Recovery of the cell voltage was also observed after the indenter was removed. Cell type B, shown in Fig. 10 (right), exhibited energetic failure accompanied by full rupture of the cell can and ejection of the electrode jelly roll. This may be due to the increased confinement of the jelly roll due to the solid core, which does not allow for easy escape of pressurized gasses that form during the abuse test. While this could also be attributed to different cell chemistries, the energetic nature of the cell disassembly of cell type B is more consistent with the differences in cell design. The concerning aspect presented here is not that the two cells showed different behavior at an elevated temperature, but that they changed in significantly different ways from the ambient temperature experiments, with failure mode of cell A becoming reliably less energetic at 60 °C and the failure mode of cell B becoming significantly more energetic and vigorous at 60 °C.

At elevated temperatures the data for cell A shows similarity to that reported by Jones et al. [12] in that there appears to be internal short circuit generation caused by the deformation of the cell. Functionally, the mechanism for this can be seen in Fig. 6. Near the surface of the cell, where the electrodes have undergone the greatest amount of deformation there is sufficient compression of the electrode layers until they are no longer physically distinct from one another and a short circuit point is created. (It should be noted that as some rupturing of the can occurred in all cases, leaving the possibility that some of the observed shorting occurred at the point of puncture.) The work here, however, also shows that there were significant differences owing both to changes in the temperature at which the puncture was performed as well as the internal construction of the cell. The presence of the solid core in particular appears to provide for a much more dramatic shorting event. Fig. 6 (right) shows that the compression of the electrode layers may be partially responsible for the short circuit. The differing reactions may be explained by the different ways the two cell constructions react to a softening of the polyolefin separator, which are known to undergo degradation of mechanical properties under elevated temperatures [20–22]. The expected mode of failure for this mechanical indentation is a loss of electrical separation by compression of the electrode layers during mechanical deformation. As more deformation is required to see an energetic short circuit event in cell A, weakening of the separator allows very localized relatively high impedance short circuit points to occur within the electrode layers, creating the mild cell failure observed. The electrode layers in cell B, meanwhile are compressed between the central core and the indenting rod, so that any softening or other weakening of the separator material can lead to a more dramatic failure as the electrode layers are compressed together.

Fig. 11 shows the cell voltage data from Fig. 11 (left) (cell type A tested at 60 °C) plotted along with its corresponding load profile to observe how much of an impact the puncturing of the cell had on the observed short circuit event. The data, collected at a 5 Hz sample rate, near the initial shorting event (left) show that the initial event and the partial puncture of the cell, seen as the sudden drop in load, occur simultaneously. The full duration of the voltage and load profiles (right), however, show that there is little to no voltage recovery when all loading from the blunt rod is removed, while the cell can be seen continuing to discharge. This shows that while the puncture of the cell may have an impact on the total short circuit impedance, and the damage that occurs during the puncture may help to usher in the short, much of the event is occurring internal to the cell.

The effect of cell construction on mechanical testing results was illustrated as well by tests performed on the 3 Ah pouch cells in both horizontal and vertical orientations (Fig. 12). Relatively lower peak temperatures (200–250 °C) and slightly lower rates of temperature rise were observed during the runaway events of these cells. This may be due largely to the change in format. Heat from the point of failure is able to more effectively spread from the point of initiation through the cell as shown by Kim et al. [23] as well as

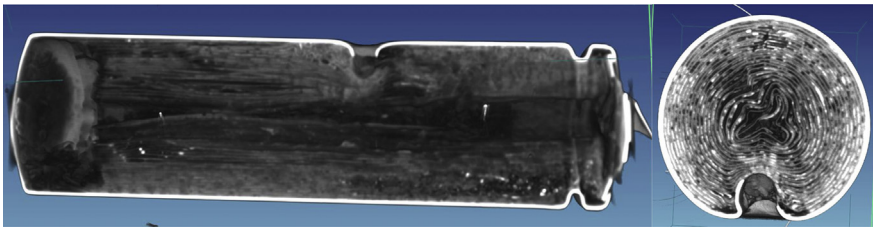

Fig. 5. CT imaging after testing detailed in Fig. 4, showing a cutaway of the entire cell (left) as well as a cross section at the point of indentation (right). This shows a significant puncture of the cell can before shorting occurred, as well as significant damage to the electrodes.

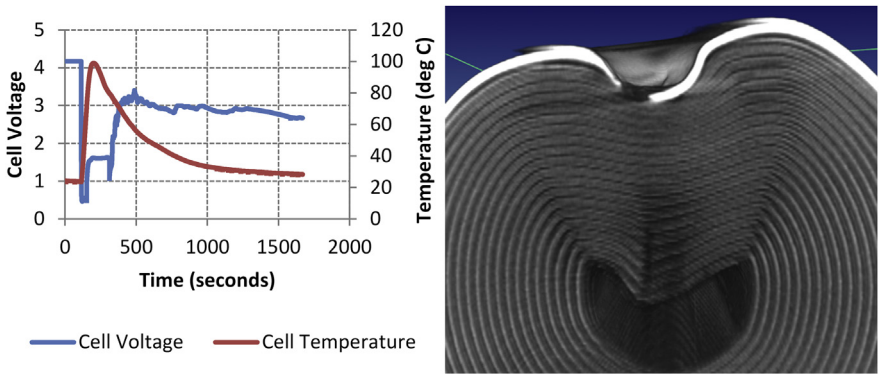

Fig. 6. Indentation normal to the cell axis conducted under the same conditions as those in Fig. 4 that produced a less vigorous shorting event. CT imaging (right) shows that the cell can was slightly ruptured, however the shorting event was likely caused by the pinching of the electrode that is seen in the outer layers of the cell. The central void also appears to provide significant space for the electrodes to collapse into with the indentation. After the indenting rod was removed a significant voltage recovery was also observed.

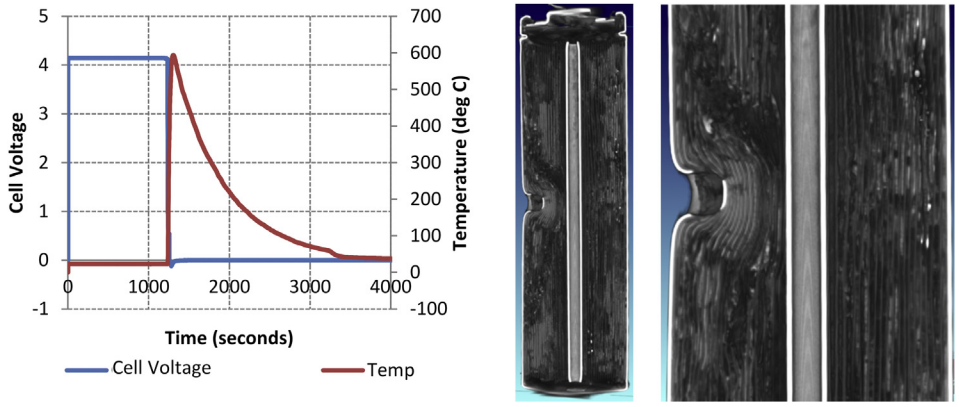

Fig. 7. Indentation normal to the cell axis on cell type B. Abrupt shorting and similar runaway temperatures to the energetic failure of cell type A were observed (see Figs. 4 and 5). (left) Venting of flammable electrolyte vapors occurred primarily from the vent at the positive cap. Significant damage to the electrode was required to cause shorting (right), however the electrode layers remained largely in their original place. The central core appears to have pinned the electrode material largely in place.

Santhanagopalan et al. [14] In both cases significant damage to the electrodes at the point of indentation was necessary to cause failure. Fig. 12 (left) shows that the shorting was vigorous enough to cause significant cell damage well away from the penetration, as the cross section shows void areas where the electrode material burned away. The testing methods used to evaluate cylindrical and rigid-case prismatic cells may however be inadequate to evaluate behaviors in flexible pouch cells. The unconstrained nature of the pouch, for example, can lead to a rapid expansion of the pouch cell and de-lamination of the electrode layers (Fig. 12 right, Supplemental 7 and 8) that may prevent a cell runaway reaction from proceeding as far as it would be able to if electrodes were forced to maintain close contact. Further, much of the puncturing of the cell through the electrode layers occurred as the pouch swelled up around the rod, making deconvolution of the failure event difficult. Other mechanical methods have been developed that may be more appropriate for this format, such as the ORNL-Motorola pinch test discussed above [7,8].

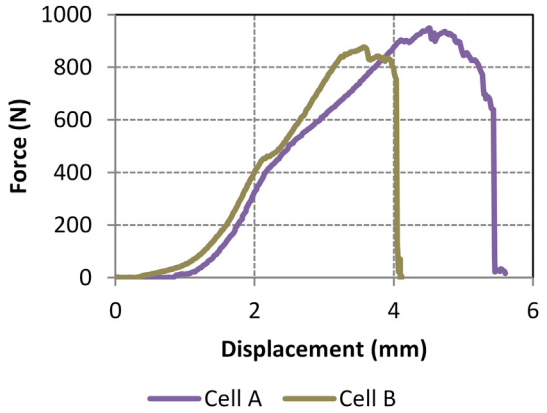

Fig. 8. Force as a function of displacement of cell A and B corresponding to data in Figs. 4 and 7. Cell B exhibited a short circuit failure at 4.05 mm while cell A ruptured and exhibited energetic failure at 5.4 mm.

The data illustrates potential variability involved with mechanical techniques. Firstly, significant damage was needed to the electrodes in most cases to initiate a short circuit event. In these cases, there is little apparent difference in the results between the blunt rod test and a traditional nail penetration test. The outcome also appears highly dependent on test parameters and other factors as well. For example, this work considered a voltage loss of 100 mV to be the initiation of a short circuit event. However, minor voltage losses were observed in many of the tests prior to the decided upon event threshold. Reducing this threshold could result in the change of consequences of shorting events. A difference in the shorting events was observed in both cells under elevated temperatures as well, with cell type A undergoing a much less vigorous short under the test parameters when tested

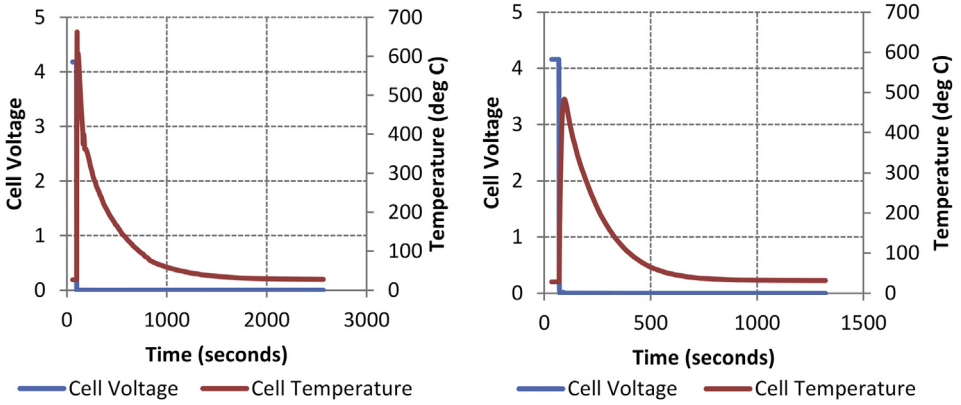

Fig. 9. Results of fast sharp nail penetration of cell type A (left) and B (right). This shows similar shorting response to the data presented in Figs. 3–6, indicating similarities in response between blunt and sharp nail testing.

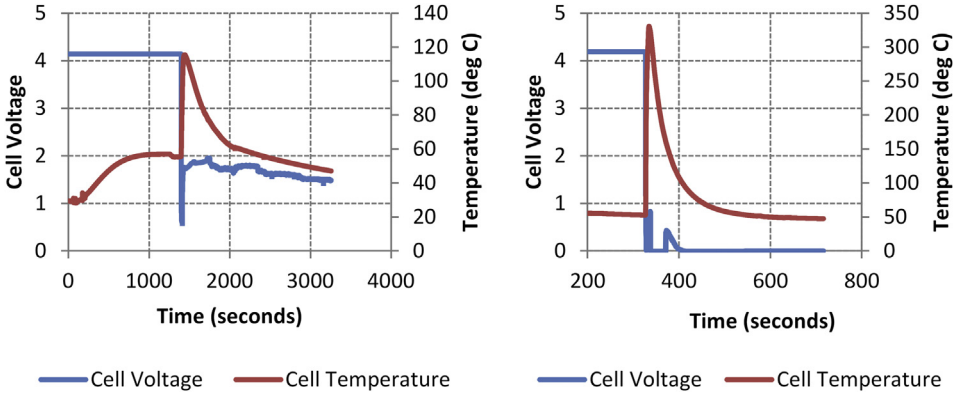

Fig. 10. (left) Indentation normal to the cell axis performed on cell type A at 60 °C. Under these conditions less vigorous shorting similar to that seen in Fig. 6 was reliably reproduced; (right) indentation normal to the cell axis on cell type B was conducted at 60 °C. In this case the cell ruptured and the cell contents were ejected.

at 60 °C, while type B under the same conditions exhibited a much more energetic shorting event.

Further, it was observed that (at least in cylindrical cells) changes in the cell construction can have an impact on the behavior under mechanical testing. Here, the presence of a solid core within the cell was observed to act to both pin the electrode jelly roll in place and allow for a more complete compression of the electrodes.

4. Conclusion

The predominant criticism of mechanical evaluation techniques is that they do not truly replicate the conditions of a field failure, but rather show how the cell behaves under an abusive condition [12,13]. The data presented illustrates some of the potential difficulties. Specifically, while the techniques evaluated show that it is possible to create a localized internal failure with mechanical

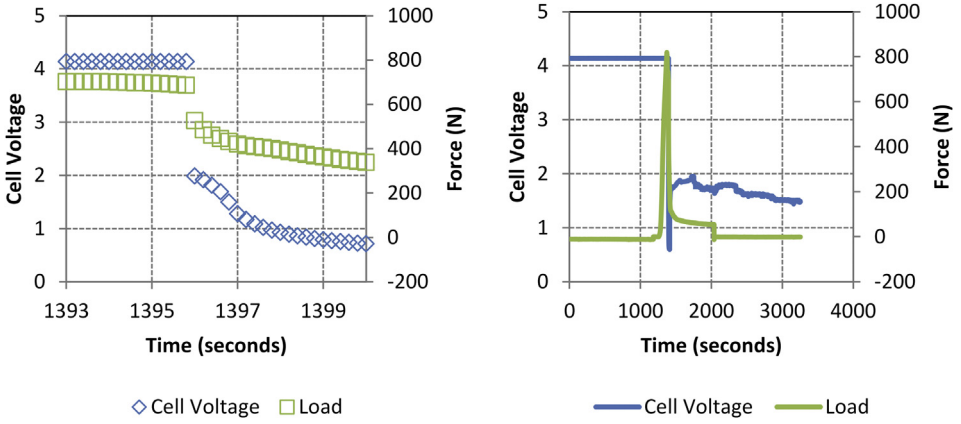

Fig. 11. Cell voltage data from Fig. 10 (left) plotted with the corresponding load profile over the 7 s surrounding the initially observed short circuit event (left) and over the duration of the test (right). The puncture and short circuit event can be seen occurring simultaneously. After removal of the load at ~2000 s there is little to no voltage recovery observed with continued self discharge afterward.

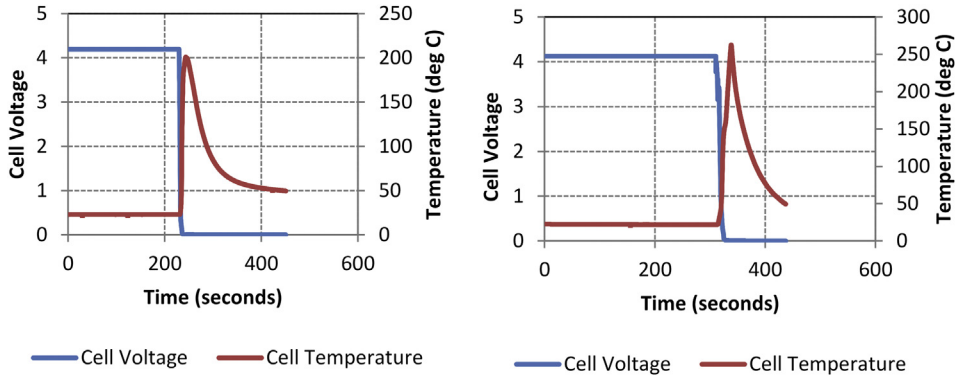

Fig. 12. Indentation into the 3 Ah pouch cells. The indenter punctured a significant distance into the cell before shorting occurred when punctured parallel to the electrode stack (left). Similar behavior is observed when testing through the face of the electrodes (right).

deformation, the outcome is highly dependent on the test conditions used, the specific construction used and how these conditions interact with each other. Because mechanical testing procedures are by design constant regardless of the battery tested, it is conceivable that cells could be physically designed to produce more benign test results, regardless of the true consequence of a failure within the cell. This is important to be aware of, as mechanical testing is still commonly used as an evaluation technique. It is important to note that the conditions under which a cell or battery (vehicle, consumer product or otherwise) is used will govern the abuse conditions presented to the energy storage system. For example, a consumer device such as a cell-phone is highly unlikely to be exposed to an event as dramatic as a sharp nail being driven through the battery. However, an on-board vehicular system could conceivably be exposed to significant mechanical deformation or intrusion during an automobile accident. While safety of lithium-ion batteries has typically focused on the impacts of spontaneous field failure, increasing numbers of electric vehicles in use could give greater weight to considering abusive modes of failure.

This illustrates the importance of understanding the behavior and impacts of mechanical abuse testing techniques. Mechanical abuse techniques are still a widely accepted method for safety and abuse response evaluation of lithium ion cells, however changes to the test conditions and even changes to the cell construction can lead to significantly different responses. How these changes impact the final result of a mechanical test are important to understand how the results from standard testing techniques may correlate to the safety performance of a cell. In the extreme case, a cell may show a relatively benign response in one test condition but be capable of an energetic, catastrophic failure. Future work would explore the specifics of how these test conditions and cell construction are interdependent with the event.

Acknowledgments

This work was performed under funding from the United States Department of Energy, Office of Vehicle Technologies.

Sandia National Laboratories is a multi-program laboratory managed and operated by Sandia Corporation, a wholly owned subsidiary of Lockheed Martin Corporation, for the U.S. Department of Energy's National Nuclear Security Administration under contract DE-AC04-94AL85000.

Appendix A. Supplementary data

Supplementary data related to this article can be found at http://dx.doi.org/10.1016/j.jpowsour.2013.08.066.

References

[1] P.G. Balakrishnan, R. Ramesh, T.P. Kumar, J Power Sources 155 (2006) 401–414.
[2] K. Wu, Y. Zhang, Y.Q. Zeng, J. Yang, Prog. Chem. 23 (2011) 401–409.
[3] L. Xia, S.L. Li, X.P. Ai, H.X. Yang, Prog. Chem. 23 (2011) 328–335.
[4] B. Scrosati, J. Garche, J. Power Sources 195 (2010) 2419–2430.
[5] E. Darcy, J. Power Sources 174 (2007) 575–578.
[6] A. Sheidaei, X.R. Xiao, X.S. Huang, J. Hitt, J. Power Sources 196 (2011) 8728–8734.
[7] W. Cai, H. Wang, H. Maleki, J. Howard, E. Lara-Curzio, J. Power Sources 196 (2011) 7779–7783.
[8] H. Maleki, J.N. Howard, J. Power Sources 191 (2009) 568–574.
[9] C.J. Orendorff, E.P. Roth, G. Nagasubramanian, J. Power Sources 196 (2011) 6554–6558.
[10] Y.E. Hyung, M. Anil, M. Rona, B. Barnett, S. Sriramulu, in: 220th ECS Meeting, Boston, MA, 2011.
[11] D.H. Doughty, C.C. Crafts, Sandia National Laboratories, Albuquerque, NM, 2006.
[12] H.P. Jones, J.T. Chapin, M. Tabaddor, in: Proceedings 4th IAASS Conference Making Safety Matter, 2010, p. 5.
[13] J. Loud, S. Nilsson, Y.Q. Du, On the Testing Methods of Simulating a Cell Internal Short Circuit for Lithium Ion Batteries, IEEE, New York, 2002.
[14] S. Santhanagopalan, P. Ramadass, J. Zhang, J. Power Sources 194 (2009) 550–557.
[15] H.-b. Wei, Y. Song, C.-j. Wang, Y. Zhao, Battery Bimon. 39 (2009) 294–295295.
[16] L. Greve, C. Fehrenbach, J. Power Sources 214 (2012) 377–385.
[17] E. Sahraei, J. Campbell, T. Wierzbicki, J. Power Sources 220 (2012) 360–372.
[18] J.A. Jeevarajan, in: IECEC 2010, 2010. Nashville, TN.
[19] E.P. Roth, in: Battery Safety and Abuse Tolerance at the 212th ECS Meeting, 2008, pp. 19–4141.
[20] E.P. Roth, D.H. Doughty, D.L. Pile, J. Power Sources 174 (2007) 579–583.
[21] X.S. Huang, J. Solid State Electrochem. 15 (2011) 649–662.
[22] S.S. Zhang, J. Power Sources 164 (2007) 351–364.
[23] G.-H. Kim, K. Smith, J. Ireland, A. Pesaran, J. Power Sources 210 (2012) 243–253.